Determination of the Surface Corrugation Amplitude from Classical Atom Scattering

W. W. Hayes*
Physical Sciences Department, Greenville Technical College, Greenville, South Carolina 29606, USA
J. R. Manson†
Department of Physics and Astronomy, Clemson University, Clemson, South Carolina 29634, USA
(Received 25 January 2012; published 10 August 2012)

The energy landscape of an atomic or molecular projectile interacting with a surface is often described in terms of a corrugation function that gives the classical turning point as a function of position vector parallel to the surface. It is shown here that the relative height variation of the corrugation function for scattering of atoms under classical conditions can be determined by a measurement of the maximum intensity in energy-resolved scattering spectra as a function of surface temperature. This is demonstrated by developing a semiclassical quantum theory of atomic scattering from corrugated surfaces and then extending the theory to the classical limit of large incident energies and high surface temperatures. Comparisons of calculations with available data for Ar atom scattering determine the corrugation amplitude for a molten In surface to be about 29% of the mean interparticle spacing in the bulk liquid.

DOI: 10.1103/PhysRevLett.109.063203 PACS numbers: 34.35.+a, 34.50.−s, 82.20.Rp, 82.45.Jn

Determining the surface energy landscape for the interaction of atoms or molecules with a surface is an important first step for predicting the results of scattering measurements as well as for predicting chemical reactions and catalysis. The energy landscape is essentially the interaction potential energy at the classical turning point plotted as a function of displacement parallel to the surface. A class of experiments that has been particularly successful at determining energy landscapes is scattering of well-defined beams of atoms from surfaces. Most such experiments have been carried out using He atoms in the quantum mechanical regime of low energies and target temperatures [1,2] where, in the best of cases, remarkable precision can be obtained. [3] However, much useful work has been done using heavier rare gas atoms as projectiles with beam velocities and target temperatures large enough that the scattering becomes governed completely by classical mechanics [4].

The purpose of this Letter is to show that useful information about the surface energy landscape, namely the average corrugation amplitude, can be obtained through a straightforward measurement of the temperature dependence of the energy-resolved scattering spectra taken in the classical regime.

In the classical mechanical regime, all quantum features are suppressed and the energy-resolved spectra appear typically as broad peaks characterized by a width that increases with the square root of the surface temperature. In the classical limit, the coherence of the surface structure becomes less important and the energy-resolved spectra for both ordered and amorphous surfaces appear similar, although the structure of ordered surfaces can exhibit rainbow features [5–9].

However, although energy-resolved spectra taken at fixed angles in the classical regime give the appearance of being insensitive to local surface structure, we would like to point out that a measurement of the most probable intensity of the typically observed inelastically broadened structure can give a measure of the average corrugation amplitude of the energy landscape. That this is the case is readily observed by comparing two different theoretical equations for the transition rate $w(\mathbf{p}_f, \mathbf{p}_i)$ describing differential cross sections in the classical limit for scattering of a projectile from the initial state of momentum $\mathbf{p}_i$ to a state of momentum $\mathbf{p}_f$. These two expressions represent the extremes of a surface that is highly corrugated or one that is regarded as being flat except for small time-dependent thermal corrugations.

A highly corrugated surface is represented by the scattering of a projectile of mass m by a collection of discrete scattering centers of mass M_S that are initially moving with an equilibrium distribution of velocities at temperature T_S [10,11]

$$w(\mathbf{p}_f, \mathbf{p}_i) \propto \sqrt{\frac{1}{4\pi k_B T_S \Delta E_0}} |\tau_{fi}|^2 \exp\left\{-\frac{(E_f - E_i + \Delta E_0)^2}{4 k_B T_S \Delta E_0}\right\}, \quad (1)$$

where $\Delta E_0 = (\mathbf{p}_f - \mathbf{p}_i)^2/2M_S$ is the recoil energy in a binary collision, k_B is Boltzmann's constant and τ_{fi} is a transition matrix element determined by the interaction potential.

When viewed as a function of final energy E_f the transition rate of Eq. (1) usually appears as a single-peaked structure whose shape is dominated by the Gaussian-like exponential. The temperature dependence of the width is

largely due to the factor of T_S in the argument of this exponential, which leads to an approximate $\sqrt{T_S}$ dependence on the full width at half maximum (FWHM) typical of classical scattering. The most probable intensity occurs when the argument of the exponential vanishes. Thus the temperature dependence of the most probable intensity is governed by the prefactor which goes as $1/\sqrt{T_S}$.

The transition rate for a surface having no static corrugation, but which undergoes small time-dependent thermal displacements due to the underlying motions of the atoms in the bulk is [12–14]

$$w(\mathbf{p}_f, \mathbf{p}_i) \propto \frac{1}{(4\pi k_B T_S \Delta E_0)^{3/2}} |\tau_{fi}|^2 \times \exp\left\{-\frac{(E_f - E_i + \Delta E_0)^2 + 2v_R^2 \mathbf{P}^2}{4k_B T_S \Delta E_0}\right\}, \quad (2)$$

where $\mathbf{P}$ is the component parallel to the surface of the momentum transfer vector $\mathbf{p} = \mathbf{p}_f - \mathbf{p}_i$ and the parameter v_R having dimensions of speed is a weighted average over the distribution of phonon velocities at the surface [12].

Equation (2) differs from Eq. (1) in that it has an added Gaussian-like factor in $\mathbf{P}^2$ and the envelope prefactor is raised to the 3/2 power as opposed to the square root. For most conditions, Eq. (2) is also a single-peaked function of the final energy E_f with the most probable intensity occurring at the final energy E_f corresponding to a minimum of the argument of the exponential. The temperature dependence of the most probable intensity will be approximately that implied by the prefactor, which has the functional dependence given by $1/T_S^{3/2}$. A temperature dependence behaving very nearly as $1/T_S^{3/2}$ has been verified in experiments using the two different projectiles ^{4}He atoms and D_2 molecules, both having similar mass, scattering under classical conditions at hyperthermal energies from a clean Cu(001) surface [15].

Comparison of the most probable intensities exhibited by Eqs. (1) and (2) shows that there is a very clear difference in temperature dependence, with the intensity of a strongly corrugated surface behaving as $1/T_S^{1/2}$ while that of an uncorrugated surface having the much stronger dependence behaving approximately as $1/T_S^{3/2}$. A logical conclusion is that a moderately corrugated surface should exhibit a temperature dependence somewhere between these two extremes [16–18]. Consequently, a measurement of the temperature dependence under conditions of most probable intensity can be used to extract the strength of the corrugation when experimental measurements are compared with appropriate theory as we demonstrate in this Letter.

Although the expressions in Eqs. (1) and (2) are classical they are readily obtained by starting from fundamental quantum mechanics and then taking the classical limit of large numbers of phonon quanta exchanged [12,14]. Although the result can be obtained using several different formalisms, a satisfactory starting point is the generalized Fermi "golden rule"

$$w(\mathbf{p}_f, \mathbf{p}_i) = \frac{2\pi}{\hbar}\left\langle \sum_{\{n_f\}} |T_{fi}|^2 \delta(\mathcal{E}_f - \mathcal{E}_i)\right\rangle, \quad (3)$$

where T_{fi} is the transition matrix element taken between final and initial states of the system of projectile plus target surface, $\mathcal{E}_i$ and $\mathcal{E}_f$ are the initial and final global energies of the entire system, and $\hbar$ is Planck's constant. The angular brackets are an average over all initial states of the surface and the $\sum_{\{n_f\}}$ indicates a sum over all final states of the target.

The transition matrix can be evaluated in the semiclassical eikonal approximation for a strongly repulsive hard wall barrier located at the position $z = \xi(\mathbf{R})$, where $\xi(\mathbf{R})$ is the corrugation function [19,20]

$$T_{fi} = ie^{i\delta_f} \frac{\hbar p_{fz}}{mL} \frac{1}{L^2} \int d\mathbf{R} e^{-i\mathbf{P}\cdot\mathbf{R}/\hbar} e^{-i\Delta p_z \xi(\mathbf{R})/\hbar} e^{i\mathbf{p}\cdot\mathbf{u}(\mathbf{R},t)/\hbar}, \quad (4)$$

where Δp_z is the component of $\mathbf{p}$ normal to the surface, $\mathbf{u}(\mathbf{R}, t)$ is the displacement of the surface due to thermal vibrations, and L^2 is the area of integration. The sum and average over target states in Eq. (3) are carried out using the Glauber–Van Hove transformation [21,22], which leads to expressions involving the displacement-displacement correlation function. The classical limit arises when the recoil energy ΔE_0 is large, and in this limit the transition rate becomes

$$w(\mathbf{p}_f, \mathbf{p}_i) = \left(\frac{p_{fz}}{mL}\right)^2 \frac{2\pi\hbar}{\sqrt{4\pi\Delta E_0 k_B T_S}} \exp\left\{-\frac{(E_f - E_i + \Delta E_0)^2}{4\Delta E_0 k_B T_S}\right\} \frac{1}{L^4} \int d\mathbf{R} \int d\mathbf{R}' e^{-i\mathbf{P}\cdot(\mathbf{R}-\mathbf{R}')/\hbar} e^{-i\Delta p_z[\xi(\mathbf{R})-\xi(\mathbf{R}')]/\hbar} \times \exp\left\{-\frac{\Delta E_0 k_B T_S (\mathbf{R} - \mathbf{R}')^2}{2\hbar^2 v_R^2}\right\}. \quad (5)$$

The leading terms in Eq. (5) are identical with the transition rate of Eq. (1), showing that if the displacement correlations arising from the flat surface are ignored the transition rate becomes that of Eq. (1) for a discrete surface. Alternatively, if the corrugation function $\xi(\mathbf{R})$ is set equal to a constant in Eq. (5), corresponding to a flat surface, then the spatial integrals become trivial and the result is just that of Eq. (2) originally due to Brako and

Newns [12]. The factors of p_{fz} are identified with the transition matrix τ_{fi} of Eq. (2) in the hard repulsive wall limit.

Equation (5) is an extension of the extreme limits of expressions (1) and (2) and can be used to interpolate between these for surfaces that are moderately corrugated, and it is valid for periodic or amorphous surfaces. As an example, Ar scattering from the amorphous molten metal surface of In will be considered here because that is the only experimental data available with full temperature-dependent measurements [23,24].

For treating classical scattering, in which there is no quantum mechanical interference arising from waves reflected from different parts of the surface, the integrals in Eq. (5) can be limited to a single typical scattering center of the surface. For the corrugation describing the interaction of an incoming Ar atom with liquid In we choose a two-dimensional sinusoidal function

$$\xi(\mathbf{R}) = ha\cos\left(\frac{2\pi R}{a}\right), \tag{6}$$

where a is chosen to be the average interatomic spacing in the bulk liquid, $\mathbf{R}$ is the two-dimensional displacement parallel to the surface and R is its magnitude which ranges from zero to $a/2$. This leads to a corrugation profile for a typical surface atom with a trough-to-crest height of $2ha$, or a root mean square elevation of $ha/\sqrt{2}$.

Figure 1 shows results of calculations with the transition rate of Eq. (5) using the corrugation function of Eq. (6), after conversion to the differential reflection coefficient. The solid curve shows the most probable intensity plotted as a function of surface temperature T_S. The open circle points are the experimental data for in-plane Ar scattering from In with the incident and detector angles equal to 55° from the normal and an incident energy of 42 kJ/mol (0.44 eV). Also shown as a dashed curve is the $1/\sqrt{T_S}$ behavior of the discrete surface expression of Eq. (1) and as a dotted curve the nearly $1/T_S^{3/2}$ behavior of the smooth surface expression of Eq. (2). The value of v_R is chosen to be 450 m/s, the same value obtained from an analysis of this data using the smooth surface model of Eq. (2) [25].

A least-squares fit of the calculations to the data points gives a corrugation factor $h = 0.29$, which for the In interatomic distance of $a = 3.14$ Å gives a corrugation amplitude $ha = 0.91$ Å for a typical In atom at the liquid surface. The rms deviation of the fit is 0.0047, which implies that the standard deviation uncertainty in the amplitude h is less than 3%.

Although the ability to extract the corrugation parameter from a simple measurement of the most probable scattered intensity as a function of surface temperature is the important result of this Letter, in order to make this result convincing the same theory must explain all available data. This is shown in Figs. 2–4, which exhibit an energy-resolved spectrum and energy-integrated angular distributions.

Figure 2 shows the energy-resolved intensity spectrum as a function of E_f from which the intensity point at $T_S = 436$ K in Fig. 1 was obtained. The dotted curve is the single-scattering calculation using Eq. (6). The dashed curve is the contribution from double scattering arising from a ring of six In atoms in the surface plane surrounding

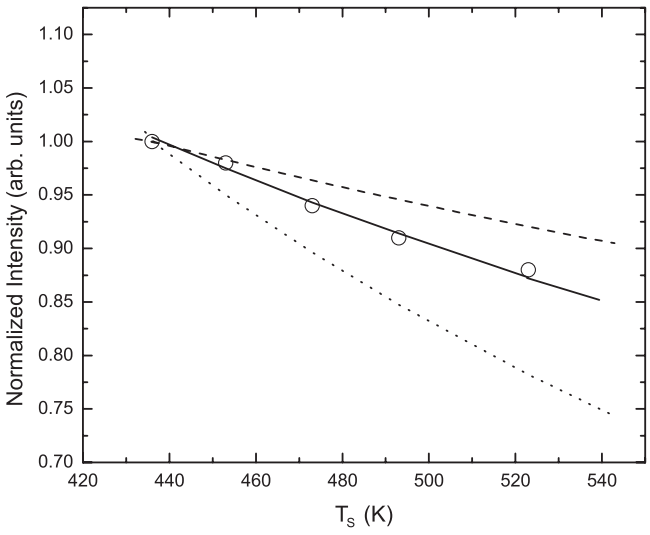

FIG. 1. Temperature dependence of the most probable intensity for a 42 kJ/mol incident beam of Ar scattering from molten In with $\theta_i = \theta_f = 55°$. The solid curve is the present calculation, the dashed curve is the result for a highly corrugated surface, and the dotted curve is the result for an uncorrugated surface. The data points are from Nathanson *et al.* [24].

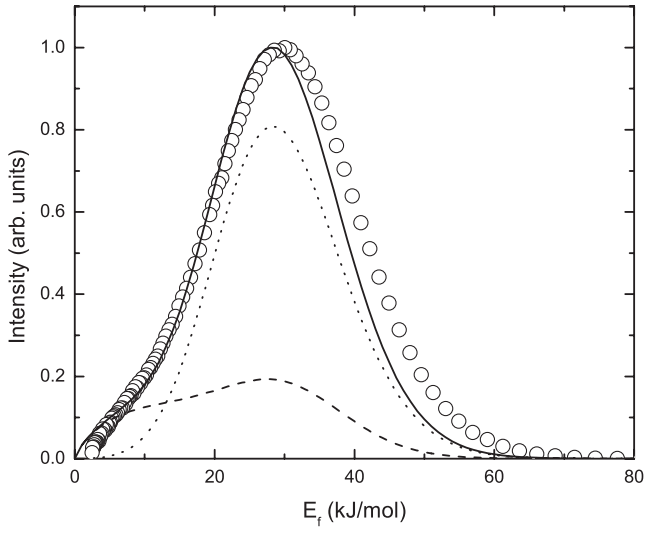

FIG. 2. Energy-resolved intensity for Ar scattering from liquid In at a temperature of $T_S = 436$ K, with $E_i = 42$ kJ/mol, $\theta_i = \theta_f = 55°$. The dotted curve is the single scattering contribution, the dashed curve is the double scattering contribution, and the solid curve is the sum of the two. Data are from Nathanson *et al.* [24].

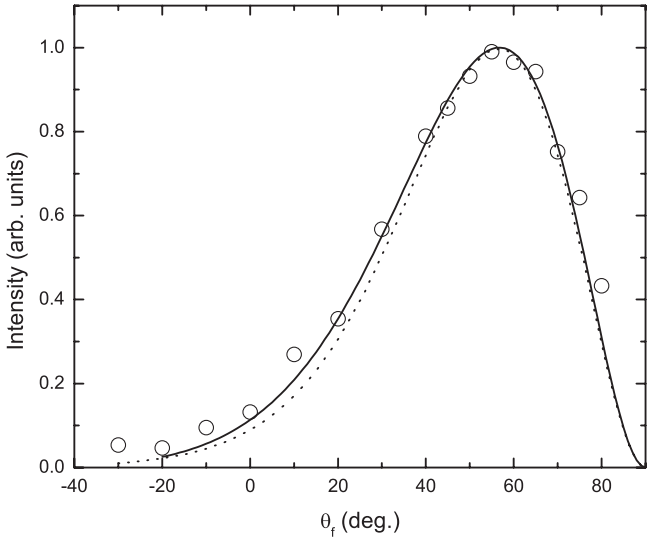

FIG. 3. In-plane angular distribution for Ar/In with $T_S = 436$ K, $E_i = 42$ kJ/mol and $\theta_i = 55°$. The data points are from Nathanson *et al.* [24].

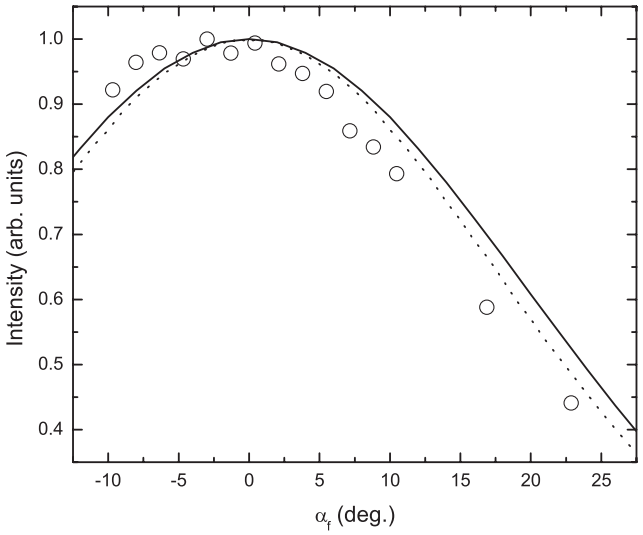

FIG. 4. Out-of-plane angular distribution Ar/In with $T_S = 436$ K, $E_i = 42$ kJ/mol and $\theta_i = \theta_f = 55°$. The data points are from Nathanson *et al.* [23].

the initial In atom at the average interparticle spacing, i.e., in a close packing arrangement [25]. Both the single scattering and single plus double scattering curves explain the experimental data well, but the double scattering contribution shows that the small shoulder feature at low E_f comes primarily from double backward scattering contributions, in which the Ar initially scatters backward from the initial In atom and then is scattered again forward into the final detector angle by a second In atom located in the region behind the first one.

Figure 3 shows a typical angular distribution measurement taken at an incident energy of 42 kJ/mol and with an incident angle $\theta_i = 55°$. Angular distributions are taken with a fixed incident angle (and the detector is at the variable angle θ_f) and measure all particles regardless of energy. The calculation using the corrugation function of Eq. (6) with $h = 0.29$ is shown as a solid curve. Also shown as a dotted curve in Fig. 3 is the smooth uncorrugated surface calculation using Eq. (2). The two calculations are quite similar, and both give a good interpretation of the experimental data shown as open circles. This illustrates a general behavior, namely, that the corrugated and uncorrugated theories give very similar shapes for the scattered spectra, since for this system they are largely dictated by phonon transfer, and that the information on the nature of the corrugation comes from examining the temperature dependence of the scattered spectra.

Figure 4 compares calculations with measurements for the out-of-plane angular distribution. The out-of-plane experiments were taken with the incident and final polar angles fixed at 55° and the intensities were taken at angles α measured perpendicularly to the sagittal scattering plane [23]. As in Fig. 3, the solid curve is the calculation for the corrugated surface using Eq. (5) and the dotted curve is for the uncorrugated surface using Eq. (2).

However, in addition to explaining all available data, as well as providing a method for extracting important information about the corrugation height, the theory developed here can answer a very fundamental question in the field of molecular beams scattering from surfaces. This is the question of the importance of inelastic phonon transfer relative to that of surface corrugation in forming the angular widths of the scattered distributions. Two quite different theoretical approaches seem to indicate that both phonons and corrugation can explain the rather large angular widths over which molecular beams can be scattered under classical conditions. The Tully [26] washboard model has been used extensively for interpreting a large amount of experimental data, and has often been shown to describe the angular spread of angular distributions in spite of the fact that it does not include a mechanism for energy transfer with the surface. Theories containing energy exchange with large numbers of phonons based on the Brako-Newns approach for a flat and uncorrugated surface similar to that of Eq. (2) have also been shown to quantitatively explain the widths of angular distributions [25]. The theory and calculations carried out here indicate that static corrugations as well as energy and momentum transfer through phonon exchange can contribute equally to similar angular spreads in the measured angular distributions. For example, in the case of Ar scattering from molten In, it is found that the corrugation effects and phonon energy transfers scatter the Ar atoms over a very similar range of final angles. This work indicates that to separate and categorize the importance of the two contributions will require extensive comparisons of experimental measurements with theory. However, important information on the average

corrugation height of the surface can be obtained from relatively simple measurements, such as the most probable intensity of the energy-resolved spectra. Furthermore, since this information is obtained from experiments carried out in the classical mechanical domain where there is no quantum mechanical interference, this conclusion holds equally well for an ordered periodic surface as for the disordered molten metal surfaces considered as illustrative examples here.

* Wayne.Hayes@gvltec.edu
†jmanson@clemson.edu

[1] G. Benedek and J. P. Toennies, Surf. Sci. **299-300**, 587 (1994).
[2] G. Benedek, M. Bernasconi, V. Chis, E. Chulkov, P. M. Echenique, B. Hellsing, and J. P. Toennies, J. Phys. Condens. Matter **22**, 084020 (2010).
[3] A. P. Jardine, S. Dworski, P. Fouquet, G. Alexandrowicz, D. J. Riley, G. Y. H. Lee, J. Ellis, and W. Allison, Science **304**, 1790 (2004).
[4] J. A. Barker and D. J. Auerbach, Faraday Discuss. Chem. Soc. **80**, 277 (1985).
[5] A. W. Kleyn and T. C. M. Horn, Phys. Rep. **199**, 191 (1991).
[6] E. Pollak and S. Miret-Artés, J. Chem. Phys. **130**, 194710 (2009).
[7] E. Pollak, J. M. Moix, and S. Miret-Artés, Phys. Rev. B**80**, 165420 (2009).
[8] E. Pollak, S. Sengupta, and S. Miret-Artés, J. Chem. Phys. **129**, 054107 (2008).
[9] J. M. Moix, E. Pollak, and S. Miret-Artés, Phys. Rev. Lett. **104**, 116103 (2010).
[10] A. Sjölander, Ark. Fys. **14**, 315 (1959).
[11] D. A. Micha, J. Chem. Phys. **74**, 2054 (1981).
[12] R. Brako and D. M. Newns, Phys. Rev. Lett. **48**, 1859 (1982); R. Brako and D. M. Newns, Surf. Sci. **117**, 42 (1982).
[13] H.-D. Meyer and R. D. Levine, Chem. Phys. **85**, 189 (1984).
[14] J. R. Manson, V. Celli, and D. Himes, Phys. Rev. B **49**, 2782 (1994).
[15] M. F. Bertino, J. R. Manson, and W. Silvestri, J. Chem. Phys. **108**, 10239 (1998).
[16] J. R. Manson, Phys. Rev. B **58**, 2253 (1998).
[17] W. W. Hayes and J. R. Manson, J. Phys. Condens. Matter**23**, 484003 (2011).
[18] E. Pollak and J. R. Manson, J. Phys. Condens. Matter **24**, 104001 (2012).
[19] U. Garibaldi, A. C. Levi, R. Spadacini, and G. Tommei, Surf. Sci. **48**, 649 (1975).
[20] V. Bortolani and A. C. Levi, Riv. Nuovo Cimento **9**, 1 (1986).
[21] R. Glauber, Phys. Rev. **98**, 1692 (1955).
[22] L. Van Hove, Phys. Rev. **95**, 249 (1954).
[23] M. Manning, J. A. Morgan, D. J. Castro, and G. M. Nathanson, J. Chem. Phys. **119**, 12593 (2003).
[24] W. R. Ronk, D. V. Kowalski, M. Manning, and G. Nathanson, J. Chem. Phys. **104**, 4842 (1996).
[25] W. W. Hayes and J. R. Manson, J. Chem. Phys. **127**, 164714 (2007).
[26] J. C. Tully, J. Chem. Phys. **92**, 680 (1990).